Int. J. Heat Mass Transfer. Vol. 35, No. 12, pp. 3431–3440, 1992
Printed in Great Britain

0017–9310/92 $5.00 + 0.00

An experimental study of conduction heat transfer in rarefied polyatomic gases

S. J. O'SHEA† and R. E. COLLINS
Department of Applied Physics, University of Sydney, N.S.W. 2006, Australia

(*Received* 4 *January* 1991 *and in final form* 9 *December* 1991)

Abstract—Experimental data have been obtained for the conduction heat transfer through a rarefied polyatomic gas (benzene or n-hexane) in a concentric cylindrical geometry. The results are of direct relevance in evacuated solar collector technology. The data were fitted to within 7% over the whole transition region by a simple semi-empirical equation, previously used for monatomic gases. A Monte Carlo simulation of the system was undertaken to obtain heat conduction and temperature profiles over the transition region in benzene and n-hexane gases.

1. INTRODUCTION

A SOLAR thermal collector converts solar radiation into thermal energy. Energy losses from the collector can occur by the physical processes of conduction, convection and radiation. Radiative energy losses can be reduced by decreasing the emittance of the solar adsorbing surface. It is possible to design a surface with low emittance for thermal radiation, whilst still maintaining a high absorptance for solar radiation. Such a surface is termed optically 'selective' [1]. Further reductions in the energy losses from solar collectors can be achieved by reducing conduction and convection losses. A transparent cover for the adsorbing surface is a feature of most solar collector designs. Maximum reduction occurs when the space surrounding the selective surface is evacuated. In a practical device it is only realistic to achieve this with a vacuum envelope of cylindrical geometry [2]. Such a device is called an evacuated tubular collector.

The evacuated solar collector developed at Sydney University is of a Dewar type construction. Figure 1 shows schematically the main features of this collector. Two glass tubes are mounted concentrically with the intervening space evacuated. The selective surface is deposited onto the outer (vacuum) surface of the inner glass tube by d.c. magnetron sputtering [3]. The top layer of the selective surface developed at Sydney University is the absorber layer and consists of a graded stainless steel–carbon cermet with amorphous hydrogenated carbon at the vacuum interface. A copper base layer provides the low emittance surface. Prior to the final vacuum sealing of the assembled collector tube, the collector is baked under vacuum at 500°C to outgas all the surfaces. Two 'standard' sized tubes are made: (i) inner tube radius 30 mm, length 1.4 m; and (ii) inner tube radius 44 mm, length 1.7 m.

The selective surface in a typical Sydney University collector tube has an emittance of ~0.04 at 100°C and an absorptance of ~0.92 [4]. The combination of this surface, and the vacuum insulation, results in very low thermal losses. Typically, stagnation temperatures of ~300°C are observed in non-concentrated sunlight. (Stagnation refers to the condition when no heat is being extracted from the collector and hence the thermal heat losses equal the incident solar energy input.) The existence of such a high stagnation temperature implies an ability for these collectors to supply heat with reasonable efficiencies at temperatures greater than 100°C. The lower losses from evacuated tubular collectors can also result in improved performance of these devices at temperatures less than 100°C, and under adverse environmental conditions.

The higher stagnation temperature possible in these tubes can, however, constitute a significant dis-

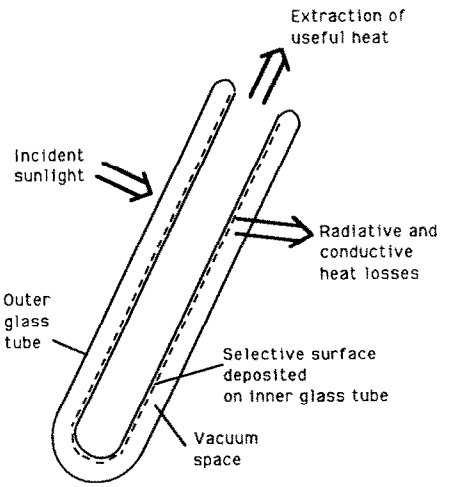

FIG. 1. Schematic diagram of an evacuated tubular solar collector.

†Present address: Engineering Department, Cambridge University, Cambridge CB2 1PZ, U.K.

NOMENCLATURE

A	area
C_V	molar heat capacity
C_w	heat capacity of water
dT	experimentally measured temperature difference
$dT(0,0)$	value of dT at $\dot{Q} = 0$
E^{vib}	energy in the vibrational modes
G	geometry factor in continuum heat loss
k	Boltzmann constant
Kn	Knudsen number
l	length of cylinders
m	mass of gas molecule
$\dot{m}$	mass flow rate
M	molar weight
P	gas pressure
Q	heat loss
Q_c	conduction heat loss in continuum region
Q_{fm}	conduction heat loss in free molecule region
$\dot{Q}$	measured power loss
r	radius of cylinder
r_c	characteristic length
R	gas constant
T	gas temperature
V_n	approximate number of excited vibrational modes
Z	collision number.

Greek symbols

α	accommodation coefficient
$\bar{\alpha}$	mean accommodation coefficient
δ	inverse Knudsen number
ΔT	temperature difference across gas
Δx	separation distance between two surfaces
θ	characteristic vibrational temperature
λ	gas thermal conductivity
λ_f	mean free path
σ^2	collision cross-section.

Subscripts and superscripts

i	inner cylinder
int	internal
o	outer cylinder
rot	rotational
tran	translational
vib	vibrational.

advantage in low temperature systems. Higher temperatures can pose significant safety hazards and may result in the accelerated degradation of system components. Overtemperature protection of a system usually involves both cost and performance penalties. Clearly it would be desirable to incorporate features integral to the collector tube itself which reduced the stagnation temperature without adversely affecting the high efficiency of the collector at low temperatures.

A method of achieving this limitation in the collector operating temperature has been developed in this laboratory [5]. Specifically, a small amount of condensable gas is introduced into the collector during manufacture. At low temperatures most of the gas remains adsorbed onto the selective surface of the inner tube, and the vacuum in the collector is at a high level. The collector therefore operates normally with very little heat loss to the surroundings. As the temperature of the selective surface increases, more gas molecules are desorbed from the surface. This degrades the vacuum space and results in significant heat losses from the inner tube surface by gas conduction through the annular space between the glass tubes of the collector. The key to the success of this approach is to make the 'thermal switch' (that is, the temperature dependence of the collector heat loss) operate over a narrow range of temperatures in order that the low temperature performance of the system is not compromised. To achieve this the desorption of gas molecules from the selective surface should be strongly dependent on temperature. In addition, heat losses through the low pressure gas must be significant.

Evacuated collector tubes using the desorbable gas method of temperature limitation (henceforth called temperature limited evacuated collectors) have been constructed [5]. Some typical data for the heat loss characteristics of these tubes are shown in Fig. 2. Note the significant reduction in the stagnation temperature as the collector is dosed with increasing amounts of

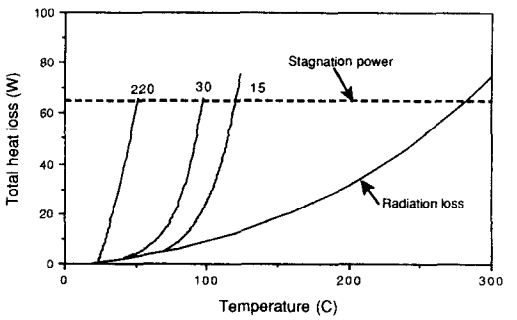

FIG. 2. The temperature dependence of the total radial heat loss in an evacuated solar collector tube dosed with various amounts of benzene vapour (shown on the graph in units of 10^{17} molecules). The data for the above graph were obtained on a non-standard sized tube with a stagnation power of ~65 W. The temperature shown refers to the temperature of the inner tube. The outer tube surface was maintained at 20°C.

gas. There are three distinct but interrelated problems involved in the operation of the system—the adsorption of gases onto thin films; the relationship between the film structure and the gas adsorption process; and the conduction heat transfer between the inner and outer tubes of the collector. The adsorption problem has been addressed elsewhere [5]. This paper addresses the heat conduction process.

The pressure range over which a typical temperature limited collector tube operates ($\sim 10^{-4}$ torr to $\sim 10^{-1}$ torr) corresponds to a Knudsen number (Kn) range of ~ 100 to ~ 0.1, where Kn is defined as [6]

$$Kn = \frac{\lambda_f}{r_c} = \frac{kT}{\sqrt{2}\pi\sigma^2 P r_c} \quad (1)$$

where λ_f is the mean free path of a gas molecule, r_c is some characteristic length (in this case the radial distance between the inner and outer cylinders), σ^2 is the collision cross-section, k is Boltzmann's constant, P is the gas pressure and T is the gas temperature. It is seen that a temperature limited collector operates over the free molecule region and well into the transition region. The heat conduction problem is therefore not simple because of the general difficulty in solving molecular transport problems in the transition region. Moreover, the desorbable gases of use in the temperature limited collector consist of large polyatomic molecules, which complicates the analysis. Previous experimental heat conduction studies in the transition region have been limited to simple molecules, such as nitrogen [7] and monatomic gases [6, 8]. In this work experimental data and Monte Carlo results are presented for heat conduction transfer through benzene and n-hexane over the whole transition range of the Knudsen number. The geometry of the collector tube is that of concentric cylinders, although it should be noted that the curvature of the system is always small. It should also be stressed that there is no provision for control of the surface conditions. Therefore, when theory and experimental data are compared the emphasis is simply to demonstrate the applicability of theoretical expressions to engineering problems involving polyatomic gases.

2. EXPERIMENTAL

Conduction heat losses are measured by a calorimetric method. Water is circulated through the inner tube of the solar collector and the difference between the inlet and outlet temperatures is used to determine the heat loss along the tube. End loss effects are negligible due to the adoption of a guarded design and temperature drops across the glass walls are readily accounted for. A feature of the design is the maintenance of near isothermal conditions along the inner and outer tubes of the collector. This method gives accurate data for the heat loss even at low pressures and small radial temperature gradients.

The experimental arrangement is shown in Fig. 3. The evacuated collector tube is connected to a high vacuum pump and an associated gas handling system. There are no O-ring seals in that part of the apparatus which is valved off from the pumps during an experiment. This significantly reduces the outgassing rate of the system. The pressure in the sealed off section increases at a rate of less than 3×10^{-6} torr h^{-1}. Capacitance manometers (MKS type 127A baratron, accuracy is 0.2% of reading, useful resolution is 0.2 mtorr for a 1 torr baratron and 10 mtorr for a 100 torr baratron) are used to measure the system pressure from 10^{-2} torr to 100 torr. A spinning rotor gauge (Leybold Viscovac VM211, accuracy is 3% of reading, useful resolution is 1×10^{-7} torr) is used to measure pressures below 10^{-2} torr. The reading of each MKS baratron is corrected by the calibration data of each instrument. The base pressure in the sealed collector tube is approximately 5×10^{-6} torr.

The outside tube of the evacuated collector is enclosed within an insulated water jacket. The temperature of the water jacket is controlled from 0°C to 100°C using a Tampson TC10 circulating water bath and the temperature stability is better than 20 mK over 10 min. Thermistors monitor the water temperature at the inlet and outlet of the water jacket. A high flow pump (10 l min^{-1}) ensures that the temperature difference along the jacket is less than 0.5°C for a heat loss of 70 W.

A water circulating insert was constructed for the temperature control of the inner tube. The insert consists of three sections. A long central section is the region over which heat loss measurements are made. Water is forced through a tee junction at the base of

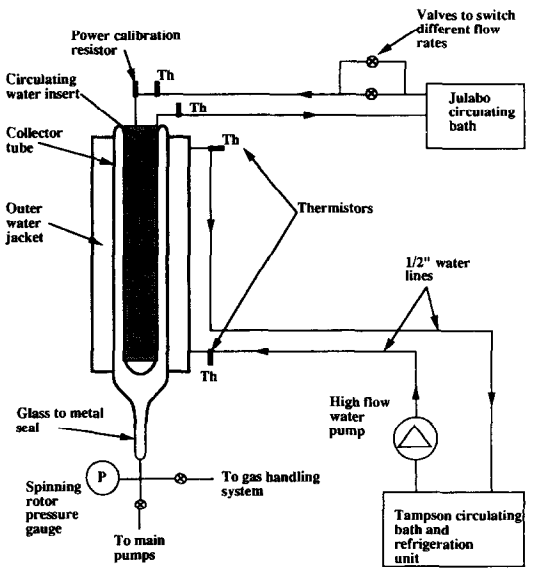

FIG. 3. Experimental arrangement for the measurement of heat losses and accommodation coefficients in an evacuated collector tube.

this section and drains through a single outlet at the top. The temperatures of the inlet and outlet are measured with thermistors. Copper wire is wound around the entire length of the central section to prevent the formation of a laminar flow layer which would give rise to a radial temperature gradient. Immediately following the inlet thermistor a 68 Ω resistor is inserted into the water flow. By applying a known power to the resistor and measuring the change in temperature between the inlet and outlet thermistors, the heat flux of the system can be calibrated using

$$\dot{Q} = \dot{m}C_w[dT - dT(0,0)] \quad (2)$$

where $\dot{Q}$ is the power/heat lost (or gained) by the system, dT is the temperature change between the inlet and outlets, $dT(0,0)$ is the value of dT when $\dot{Q}$ is zero, $\dot{m}$ is the mass flow rate of water and C_w is the heat capacity of the water. Values of $\dot{m}C$ calculated this way agree with the less accurate method of calculating $\dot{m}$ and C_w separately. Power to the resistor is supplied by a BWD 272A stabilized power supply and a four-wire measurement is made of the voltage and current. The resistor and its wires are covered with a thin layer of epoxy resin to prevent hydrolysis of the water when a voltage is applied. The important point about using equation (2) to determine heat loss is that the method is a difference technique. Temperature fluctuations in the control bath, heat losses in the pipes and radiative losses from the tube inner are all factored out when the 'zero' value of dT (i.e. $dT(0,0)$) is found prior to the admission of gas into the collector tube.

At either end of the insert are two shorter sections which serve as heat loss guards for the central section. Water is circulated in series first to the central measuring section, then to the top guard and then to the bottom guard. In this way the heat loss from the central section is almost entirely radial. It is estimated that end losses represent less than 0.5% of the measured heat loss. Another important function of the guards is to ensure that the surface under study is uniform over the entire central (measurement) section since the production process gives rise to different surfaces at the ends of the collector tube.

The temperature of the insert is controlled to better than 0.003 K by a Julabo EO6 circulating bath and all the water lines are thermally insulated. The water lines running down the inside of the insert are separated from each other and the walls by teflon spacers. This ensures that negligible heat transfer can occur between the water lines. The temperature of the inner tube is isothermal to within 2.0°C when the power loss is 70 W (this is a worst case condition). Obviously the tube can be made more nearly isothermal by increasing the water flow rate but this will decrease the resolution in the measurement of dT. Two flow rates are available in this experiment (0.011 l s^{-1} or 0.006 l s^{-1}), with the high flow rate being used when the heat loss increases above ~15 W.

The thermistors used are nominally 2 kΩ at 25°C and are encapsulated in glass. They are protected by mounting in a stainless steel tube. The thermistor resistance is measured with an HP 3455A digital voltmeter using the four-wire technique. The resolution is 0.001 Ω for resistances less than 1 kΩ and 0.01 Ω for resistances greater than 1 kΩ. Each thermistor was calibrated against a platinum resistance thermometer, which in turn had been calibrated from 0°C to 100°C with an accuracy of 0.02°C. By checking at various temperatures it is estimated that the accuracy of the temperature as measured by the thermistors is ±0.04°C over the range 10–90°C.

Three gases were used, namely helium (99.99% purity), benzene (99.7% purity) and n-hexane (99.5% purity). All gases were dried by passing through type 3A molecular sieves. Dissolved gases in the benzene and hexane were removed by the freeze-thaw method [9].

Three large (1.8 m long) collector tubes were used in the experimental study. Two of the collector tubes contained an inner tube coated with selective surface. The radial distance between the inner and outer cylinders was slightly different for each (2.65 mm and 2.1 mm). The third collector tube contained an uncoated pyrex glass inner tube. The results from this collector tube were used solely to find the accommodation coefficient for the various gases on pyrex glass. All of the collector tubes were carefully constructed to be as concentric as possible. In a typical experiment the entire collector tube is baked at 250°C for 1 h to remove adsorbed gas. The oven is then removed and the water jacket and insert put in place. The values of $\dot{m}C$ and $dT(0,0)$ are then found. Various quantities of gas may then be admitted into the system and dT measured at a given pressure. After the admission of a dose of gas the system will thermally equilibrate within 4 min.

The conduction heat loss through the gas is presented as the power which flows per unit area of the inner cylinder (units W m^{-2}). Also, since the heat loss is proportional to the temperature difference between the inner and outer walls of the collector tube (ΔT), the data is often normalized by dividing by ΔT (units W m^{-2} K^{-1}). All the data are corrected for end losses and temperature drops across the glass walls of the collector tube. Both corrections are small. The effective temperature of the gas (T) is taken as being $(T_i + T_o)/2$, where T_i is the temperature of the inner surface and T_o is the temperature of the outer surface.

3. MONTE CARLO METHOD

A quantitative description of heat loss in the transition region is difficult since the Boltzmann equation must be solved with the appropriate boundary conditions. Significant progress on the problem has only been made since about 1960. The theoretical methods developed since that time, particularly using the linearized Boltzmann equation, have been successful in describing the transport properties of stationary

monatomic gases over the whole range of Knudsen number.

There are four general means of obtaining theoretical heat loss results in the transition region. These are:

(i) direct numerical solutions of the Boltzmann equation or approximations of the Boltzmann equation;
(ii) moment methods [10, 11];
(iii) variational methods [8, 12], in which the linearized Bhatnagar–Gross–Krook (BGK) model [13] is used; and
(iv) Monte Carlo simulations [14].

All of these methods give reasonably good agreement with experimental results for monatomic gases [6], with the moment method of Lees and Liu [11] giving the best solution that can be written in a closed form. A molecular level description of heat transfer in a rarefied polyatomic gas would seem to be best approached using either the variational or Monte Carlo methods.

In this study, the direct simulation Monte Carlo method of Bird [14], is used, based on a variable hard sphere model. The treatment of internal degrees of freedom is based on the Larsen–Borgnakke model [15]. The collector tube is cylindrically symmetric so the simulation is constructed solely in terms of the radial distance from the axis of the central cylinder. The radial distance is divided into 80 cells, which in turn are divided into four sub-cells. The average value of a quantity at some radial position in the gas is found by sampling and averaging over the four sub-cells. A full description of the sampling procedure and the molecular collision model used is given in refs. [14] and [15]. Table 1 gives values for the various parameters used in the simulation. Typically about 2000 molecules are used. The hard sphere collision diameter is calculated at the stream temperature and the temperature variation of the diameter is given approximately in terms of the viscosity coefficient [10]. The only difference between the present work and the technique given in refs. [14] and [15] is that molecules with many internal degrees of freedom must be modelled, and therefore some of the collisions will be inelastic. Also, the molecular interaction will not generally be spherically symmetric. Both of these problems can be overcome to some extent.

The use of a spherically symmetric model for polyatomic molecules proves to be satisfactory because the collision dynamics are determined by a potential averaged over all molecule orientations. The orientations appear random prior to and during a collision. Detailed molecular potentials, such as that given for benzene by Evans and Watts [16, 17], are therefore unnecessary in a kinetic description of heat transfer at this level. It is best to use experimentally determined model parameters [18].

For a spherically symmetric potential the only major change brought about by the internal molecular states is that one of the collision invariants becomes the total energy rather than just the kinetic energy. In the Monte Carlo simulation, the molecule–molecule energy transfer process is described by partitioning the energy of a molecule into translational, rotational and vibrational components, which are then allowed to relax to equilibrium via the molecular collisions. The number of collisions required for the internal modes to equilibrate with the translational modes is given by rotational (Z^{rot}) and vibrational (Z^{vib}) collision numbers. The collision number has proved to be a most convenient means of presenting average molecular collision data and values of rotational and vibrational collision numbers are tabulated for many molecules [18–20]. The magnitude of Z^{vib} is strongly correlated with the frequency of the lowest vibrational mode. This occurs because vibrational–vibrational (V–V) energy transfer in the molecule is rapid so that the vibrational–translational energy transfer is approximately rate limited by the relaxation of the

Table 1. Parameters used in the Monte Carlo simulations; these represent the 'standard' case and have been chosen to represent the best available experimental data (the benzene parameters are for a collector tube baked at 300°C and the n-hexane parameters are for a collector tube baked at 500°C)

Parameters	Benzene	n-Hexane
Inner radius (m)	0.0209	0.02085
Outer radius (m)	0.0236	0.02295
Stream temperature (K)	310	310
Temperature of inner cylinder (K)	340	340
Temperature of outer cylinder (K)	280	280
Accommodation coefficient at inner	0.88	0.87
Accommodation coefficient at outer	0.89	0.914
Mass of molecule (kg)	1.295×10^{-25}	1.431×10^{-25}
Hard sphere diameter (m)	7.17×10^{-10}	8.03×10^{-10}
Viscosity coefficient	1.08	0.90
Rotational degrees of freedom	3	2
Rotational relaxation number	3.5	0.5
V_n	13.8	22.9
θ	986	760
Vibrational relaxation number	43	1

lowest vibrational mode. This is strong justification for the use of a single value of Z^{vib} even though there may be many vibrationally active states.

Rotational relaxation is more difficult to investigate experimentally. Rotational–translational energy transfer is very rapid, however, and one would expect that the rotational relaxation number (Z^{rot}) is of order unity. At room temperature all heavy molecules show a single rotational relaxation time and one can use the classical theory of rotational energy exchange [18] to show that $Z^{rot} \approx 5$ for benzene and $Z^{rot} \approx 1$ for n-hexane at room temperature. Moments of inertia can be found using spectroscopic data [21].

The amount of energy stored in the translational modes is $\frac{3}{2}kT$ per molecule. The rotational states are fully excited at the temperature used and the energy stored per molecule in these states is kT for linear molecules and $\frac{3}{2}kT$ for non-linear molecules. The energy in the vibrational states is

$$E^{vib} = k\sum_r \frac{\theta_r}{e^{\theta_r/T}-1} \quad (3)$$

which is simply expressing equation (3) in terms of vibrational mode. Benzene has 30 vibrational modes and n-hexane has 55, and the application of equation (4) to these gases is prohibitively time consuming in the simulation. Alternatively, since the absolute value of E^{vib} is the only quantity of interest, one can write

$$E^{vib} = \frac{kV_n\theta_r}{e^{\theta_r/T}-1} \quad (4)$$

which is simply expressing equation (4) in terms of only one vibrational mode, of characteristic temperature θ. This seems satisfactory in light of the very rapid V–V energy transfer process. V_n is approximately equal to the number of excited vibrational modes. The values of θ and V_n were found by fitting experimental heat capacity data [22] over the required temperature range. Using the values of θ and V_n given in Table 1 the value of E^{vib} calculated using equation (4) differs from that calculated using equation (3) by $<1.4\%$ for benzene and $<0.6\%$ for n-hexane over the temperature range from 280 to 340 K.

Collisions between the gas molecules and the boundaries are modelled using diffuse-specular accommodation coefficients. No distinction is made between internal (α^{int}) and translational (α^{tran}) accommodation coefficients because the primary aim of the simulation is to find the total heat transfer between the system boundaries.

4. RESULTS AND DISCUSSION

4.1. *The continuum region*

Figures 4, 5 and 6 summarize the experimental data obtained for benzene and n-hexane over the whole Knudsen range studied ($10^{-4} < Kn < 10$). Figure 4 demonstrates that the experimental data scales with ΔT. As expected, the heat flux is essentially constant

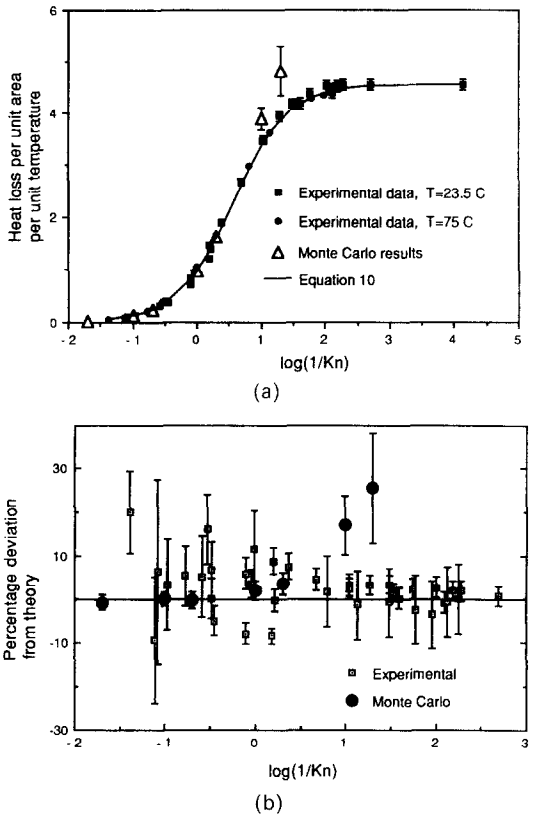

FIG. 4. A comparison of results for the conduction heat loss through benzene over the whole Knudsen range studied. The collector tube ($A_i = 0.199$ m^2, radial gap 2.65 mm) has been baked at 300°C. The heat loss is normalized by dividing by $A_i\Delta T$. (a) Normalized heat flux as a function of the inverse Knudsen number. (b) The percentage deviation of the experimental and Monte Carlo results from the results given by $1/Q = 1/Q_{fm} + 1/Q_c$.

in the continuum region ($Kn < 10^{-3}$). The conduction heat loss in the continuum region (Q_c) can be written as [23]

$$Q_c = G\lambda\Delta T \quad (5)$$

where G is a term relating to the system geometry and λ is the thermal conductivity of the gas. Expressions for G which are useful in this work are:

$$G = 2\pi l/\ln(r_o/r_i) \quad (6)$$

for heat loss between two concentric cylinders, and

$$G = A/\Delta x \quad (7)$$

for heat loss between two plane parallel plates. In these expressions, l is the length of the cylinders, r_o the radius of the outer cylinder, r_i the radius of the inner cylinder, A the area of the plates, and Δx the plate separation. Using equations (5) and (6) one can calculate, using published values of λ [22], that $G = 80 \pm 7$ m for the 2.65 mm gap collector tube and $G = 99 \pm 18$ m for the 2.1 mm gap collector tube. These values compare favourably with the experimentally determined values of $G = 77 \pm 5$ m and $G = 97 \pm 6$ m respectively. The large errors in the cal-

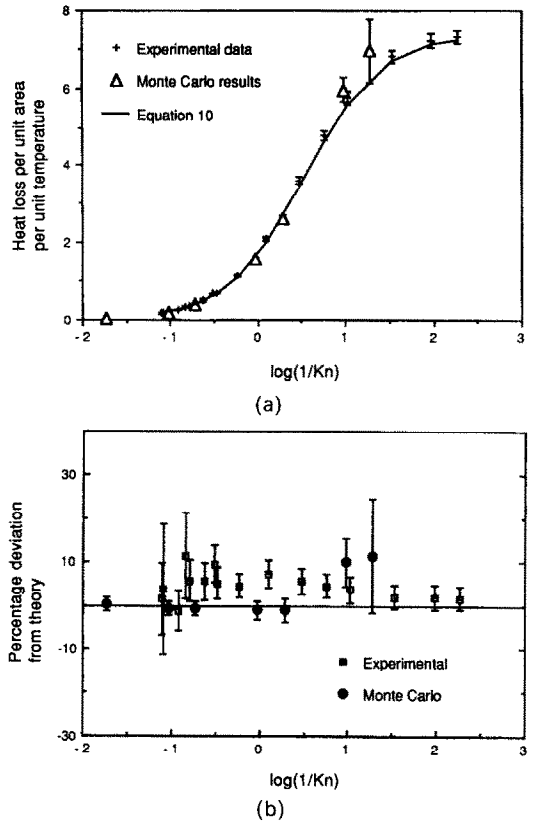

FIG. 5. A comparison of results for the conduction heat loss through n-hexane over the whole Knudsen range studied. The collector tube ($A_i = 0.198$ m^2, radial gap 2.1 mm) was baked at 500°C. The heat loss is normalized by dividing by $A_i\Delta T$. (a) Normalized heat flux as a function of the inverse Knudsen number. (b) The percentage deviation of the experimental and Monte Carlo results from the results given by $1/Q = 1/Q_{fm} + 1/Q_c$.

culated value of G result from the difficulty in obtaining accurate values of r_i and r_o. Moreover, it is unlikely that the cylinders of the collector tube are precisely concentric. The experimental value of G is therefore considered a more accurate measure of the effects of system geometry in the continuum region, and it is this value of G which will be used in all further discussions concerning the experimental data.

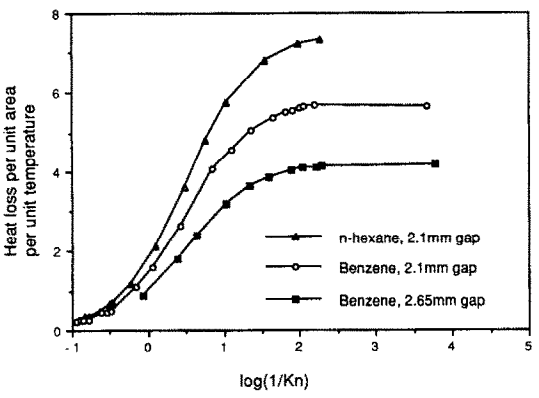

FIG. 6. Variations in the normalized conductive heat loss arising from changes in collector tube geometry and from the use of different gases. The gap refers to the radial distance between the inner and outer cylinders of the collector tube. The points represent experimental data and the lines are the results obtained from $1/Q = 1/Q_{fm} + 1/Q_c$.

4.2. *Free molecule heat loss and accommodation coefficients*

For systems which can be described using only one geometric variable, the free molecule heat conduction (Q_{fm}) can be written [6]:

$$Q_{fm} = A\left[\frac{1}{\alpha_i} + \left(\frac{r_i}{r_o}\right)^b\left(\frac{1}{\alpha_o} - 1\right)\right]^{-1} \frac{(C_V + R/2)}{\sqrt{(2\pi MRT)}} P\Delta T \tag{8}$$

where α_i and α_o are the energy accommodation coefficients at the inner and outer surfaces respectively, R is the gas constant, M is the molar weight, C_V the molar heat capacity at constant volume, and b is a constant equal to 0 for parallel plates, 1 for concentric cylinders and 2 for concentric spheres. The terms P and T relate to equilibrium properties of the gas.

The energy accommodation coefficient is defined as [24]

$$\alpha = \frac{E_{in} - E_r}{E_{in} - E_w} \tag{9}$$

where E_{in} is the energy flux of molecules incident on the surface, E_r the reflected energy flux and E_w the energy flux of the reflected molecules if the molecules were in thermal equilibrium with the wall. For polyatomic molecules the interpretation of α is complicated by the fact that the internal states of the gas molecule may accommodate with the surface to different degrees. Translational, rotational and vibrational accommodation coefficients can be defined in an analogous manner to equation (9). As one would expect the rotational states take longer to equilibrate thermally than the translational states and the vibrational states take still longer. One therefore expects that $\alpha^{tran} \geqslant \alpha^{rot} \geqslant \alpha^{vib}$ and this has been verified experimentally [25]. All values of α tend to unity as the residence time for the molecule on the surface becomes longer (that is, the temperature decreases or the gas-surface potential becomes stronger).

The low pressure method [24] is the basis of measurements of α used in this study. Experimentally it was verified that the measured free molecule heat flux (Q_{fm}) varies linearly with ΔT and the pressure. The slope of the Q_{fm} vs P plots was found by a least squares method and hence the mean accommodation coefficient $\bar{\alpha}$, defined as

$$\frac{\alpha_o\alpha_i}{\alpha_o + \alpha_i(1-\alpha_o)A_i/A_o},$$

could be found using equation (8). By finding $\bar{\alpha}$ for the all-glass collector tube, in which $\alpha_i = \alpha_o$, the accommodation coefficient for the gas on the selective surface can be found by substituting the glass accommodation coefficient for α_o. Values of the exper-

imentally determined accommodation coefficients are given in Table 2. Note that the specular–diffuse boundary condition is used in the Monte Carlo simulations rather than the energy accommodation coefficient. Loyalka and Thomas [26] have shown that either definition of α will give results within 3% for the heat transfer between parallel plates over the whole range of Knudsen number.

Benzene and n-hexane are strongly adsorbed onto both the selective surface and the pyrex [9]. One would expect that $\alpha^{int} = \alpha^{tran}$ because the molecules are certainly resident on the surface long enough for the vibrational states to equilibrate. The fact that $\alpha < 1$ suggests that α is determined by the ability of the surface to trap the incoming molecule ($\alpha^{tran} < 1$) rather than $\alpha^{int} \ll \alpha^{tran}$.

At room temperature the interaction potential between a helium gas molecule and a surface is so weak that the average gas molecule has little time to equilibrate with the surface and the energy exchange is similar to an elastic collision between two masses. The decrease in α for helium on pyrex after baking is presumably due to the loss of hydroxyl groups from the glass surface. The atomic bonding of Si–O–Si structures is stronger than that of Si–OH type structures, so that the effective mass of the dehydroxylated surface appears to increase and α to decrease. There is no apparent change in α for helium on baking the selective surface. It would seem that even though significant quantities of hydrogen, carbon monoxide and hydrocarbons are evolved from the film during a bakeout [27] and the top layer of the film becomes partially graphitic, the actual *surface* of the film has not changed significantly as far as α is concerned. Presumably the helium molecules are still colliding with carbon atoms and the effective mass of these atoms has not changed. This also appears to be the case for benzene on the selective surface.

4.3. *The transition region—results*

The experimental results for the heat loss (Q) over the transition region can be fitted by the equation [6]:

$$\frac{1}{Q} = \frac{1}{Q_{fm}} + \frac{1}{Q_c} \tag{10}$$

Table 2. Experimental values of the accommodation coefficient of helium, benzene and n-hexane on the surfaces of a collector tube

Bakeout temperature and test gas	$\bar{\alpha}$	α (selective surface)	α (pyrex)
Helium: 300°C bake	0.24 ± 0.015	0.37 ± 0.05	0.38 ± 0.03
500°C bake	0.22 ± 0.01	0.42 ± 0.06	0.29 ± 0.02
Benzene: 300°C bake	0.80 ± 0.03	0.88 ± 0.06	0.89 ± 0.04
500°C bake	0.86 ± 0.06	0.87 ± 0.07	0.99 ± 0.04
Hexane: 500°C bake	0.81 ± 0.03	—	—

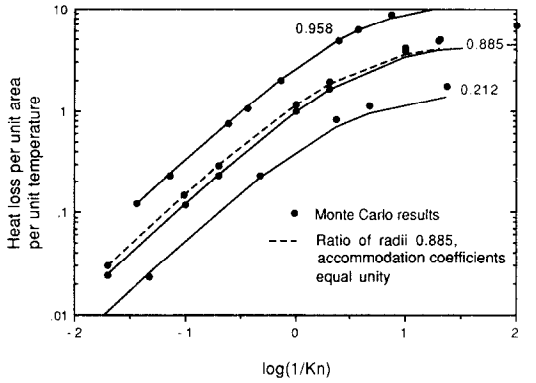

FIG. 7. The variation in the radial conduction heat loss with radius ratio r_i/r_o. The results are for the transport of heat through benzene in a concentric cylindrical geometry with $\alpha_i = 0.88$ and $\alpha_0 = 0.89$ unless otherwise noted. The mean temperature is 310 K. The lines represent data calculated from $1/Q = 1/Q_{fm} + 1/Q_c$ and the points are Monte Carlo results. The value of r_i/r_o is shown for each curve.

where the free molecule heat loss Q_{fm} is given by equation (8) and the continuum heat loss Q_c is given by equation (5). This expression is entirely empirical over the transition region. It has been found that for a monatomic gas, equation (10) is identical to that given by the moment method of Lees and Liu [11] for one-dimensional heat transfer problems. The percentage derivation of the experimental data from equation (10) is defined as $100 \times (Q^{experimental} - Q^{theory})/Q^{theory}$. Figures 4(b) and 5(b) show that the theory and experiment deviate at most by about 7% over the whole Knudsen range. One can discern a slight trend in the transition region, in that $Q^{experimental} > Q^{theory}$.

Figures 6, 7 and 8 show that equation (10) fits equally well for two quite different gases (benzene and n-hexane) and for two different sized collector tubes.

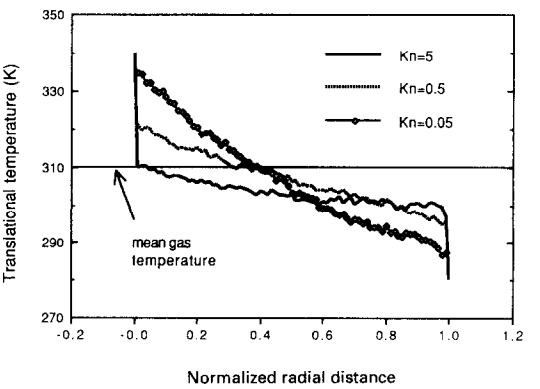

FIG. 8. Monte Carlo results for the transitional gas temperature profile in benzene between the inner and outer surfaces of a concentric cylindrical system ($r_i = 20.9$ mm, $r_o = 23.6$ mm). The radial distance is normalized such that the distance between the cylinders is unity.

Thus it appears that equation (10), which has proved useful in the study of monatomic gases, can be directly applied to the case of large polyatomic molecules.

The Monte Carlo results are also plotted in Figs. 4, 5 and 6. These results are satisfactory for $1/Kn < 10$, which suggests that the molecular model adopted is not unreasonable. For $1/Kn > 10$, the heat loss as predicted by the Monte Carlo method becomes progressively too large, which is probably due to the inherent difficulty of the Monte Carlo method in obtaining reliable data for high $1/Kn$. The Monte Carlo method provides the best quantitative means of understanding aspects of the heat loss problem that are difficult to investigate experimentally or theoretically. Results may be found for arbitrary system geometries or for non-linear problems, where ΔT is large. The temperature and density can also be found at any position in the gas. Two examples will now be given.

Figure 7 shows the variation in the heat flux between two concentric cylinders as the ratio of their radii (r_i/r_o) changes. The characteristic length used in calculating Kn is defined as $r_i \ln(r_o/r_i)$. This seems appropriate for cylindrical geometries [11]. The effect of narrowing the gap between the cylinders is to extend the pressure region over which free molecule conditions prevail, which is a useful feature for the temperature limited collector tube. The solid lines in Fig. 7 represent results calculated from equation (10). The fit to the data is worst for the small radius ratio (0.212) but becomes progressively better as r_i/r_o increases. Again, it is believed that this occurs because the statistical errors for the Monte Carlo results are not sufficiently small. In this regard it should be noted that the heat flux becomes smaller as r_i decreases.

Figure 8 shows some typical Monte Carlo results for the temperature profile between the inner and outer surfaces of a concentric cylindrical system. The temperature jump near the walls has been drawn as a solid line. In the cylindrical cases considered here, the curvature of the system causes the gas to be colder near the outer wall simply because these regions receive a proportionally higher flux of cold molecules. There is no significant difference between the translational and internal temperature profiles. Significant differences would only occur if $\alpha^{int} \ll \alpha^{tran}$ or if $Z^{int} \to \infty$ (that is, the internal modes are 'frozen').

4.4. *The transition region—discussion*

Previous experimental investigations of the conduction heat loss in a polyatomic gas over the transition region are limited to only two studies of consequence. Teagan and Springer [7] measured the heat loss and density profile between two parallel plates for nitrogen. These data are fairly sparse and there is some doubt about the accuracy of the accommodation coefficient. Semyonov *et al.* [28] measured the heat transfer through nitrogen, air and carbon dioxide in a concentric cylinder geometry. The central cylinder was a fine wire. Semyonov *et al.* also fitted all their experimental data to within ~8% using Lees and Liu's moment result [11], with a similar exerimental scatter in Q/Q_{fm} for both monatomic and polyatomic molecules.

Variational techniques have proved to be the most fruitful means of obtaining theoretical results for the transport properties of polyatomic gases over the transition region. Reasonable agreement (differences of $< 10\%$ in Q/Q_{fm}) has been obtained between theoretical expressions which have been solved numerically and the above mentioned experimental data [29, 30]. In contrast, Cipolla [31] has obtained a closed form solution for the heat transfer through a polyatomic gas between parallel plates, valid at all degrees of rarefaction. This theory was tested against the experimental data and found to be entirely unsatisfactory. The reason for this failure is not clear since the molecular model [29] and the variational technique used [8] have previously been found to give good numerical results [30].

In summary, previous experimental results have been restricted to simple polyatomic gases with two rotational states being excited. In this study, benzene and n-hexane are used as the test gases at room temperature. There is little doubt that the internal modes of such complex molecules play an important role in the heat transfer problem. However, a strong comparison between theoretical and experimental results is difficult because the small system curvature [6] and the fact that $\alpha^{int} \approx \alpha^{tran}$ render Q/Q_{fm} insensitive to the various parameters of the problem. This is not a serious shortcoming because the primary goal of this work is to calculate the heat flux at a given Knudsen number. However, it is perhaps not surprising that even a crude estimation of Q, as given by equation (10), gives a reasonable result for the present system. It is important to note that ΔT is small ($\Delta T < 80^\circ C$), so that non-equilibrium effects are not large. This, and the fact that $\alpha^{int} = \alpha^{tran}$, suggests that under such conditions simple expressions derived for monatomic gases (such as equation (10)) can also be applied to polyatomic gases. A stronger test for any theoretical description is to predict the correct temperature or density profile between the system boundaries. The Monte Carlo method offers an easy means of obtaining such data, even for large values of ΔT.

5. CONCLUSIONS

Accurate data have been obtained for the conduction heat transfer through benzene and n-hexane over the whole transition region. A concentric cylindrical geometry is used. The results were fitted to within 7% by equation (10) ($1/Q = 1/Q_{fm} + 1/Q_c$). This formula is identical to the moment method solution of Lees and Liu [11] for monatomic gases. The validity of equation (10) probably stems from the simple geometry of the problem and the fact that the system is not too far from equilibrium.

A Monte Carlo simulation of the system was under-

taken, with the energy exchange between large polyatomic molecules being described using a simple model. The results are satisfactory for both benzene and n-hexane. The simulation was used to study the effect of the Knudsen number and the radius ratio r_i/r_o on the heat loss and the temperature profile of evacuated tubes containing desorbable gas. Such data are difficult to obtain experimentally.

The accommodation coefficients (α) for helium, benzene and n-hexane were found for the selective surface and pyrex glass. Annealing the surfaces at 500°C did not change α for the selective surface but α changed markedly for the pyrex surface. This is interpreted as being due to the removal of hydroxyl groups from the pyrex surface.

The results show the considerable variation in heat flux at all degrees of rarefaction due to changes in gas type and the collector tube geometry. This is of considerable practical importance and demonstrates that:

(i) close tolerances must be maintained on the tube geometry in order that the temperature limitation of the collector tube is reproducible;
(ii) the heat flux in a temperature limited collector tube is more strongly dependent on temperature if the conducting gas has a higher continuum thermal conductivity and if the gap between the inner and outer cylinders is smaller; and
(iii) the effects of variations of the accommodation coefficient caused by annealing are negligible compared with (i) and (ii).

Acknowledgements—The authors wish to thank Professor G. A. Bird for many useful discussions and for the use of some of his Monte Carlo routines. This work has been supported by His Royal Highness Prince Nawaf bin Abdul Aziz of the Kingdom of Saudi Arabia through the Science Foundation for Physics within the University of Sydney.

REFERENCES

1. R. A. Buhrman and H. G. Craighead, *Solar Materials Science* (Edited by L. E. Murr). Academic Press, New York (1980).
2. B. Window and G. L. Harding, Progress in the materials science of all-glass evacuated collectors, *Sol. Energy* **32**, 609–623 (1984).
3. G. L. Harding, B. Window, D. R. McKenzie, A. R. Collins and C. M. Horwitz, Cylindrical magnetron sputtering system for coating solar surfaces onto batches of tubes, *J. Vac. Sci. Technol.* **16**, 2105–2108 (1979).
4. S. P. Chow, Experimental studies of all-glass evacuated collector tubes, Ph.D. Thesis, Sydney University (1984).
5. B. A. Pailthorpe, R. E. Collins and S. O'Shea, Temperature limitation in evacuated solar collector tubes, *Aust. J. Phys.* **40**, 643–658 (1987).
6. G. S. Springer, *Advances in Heat Transfer* (Edited by T. F. Irvine and J. P. Hartnett), Vol. 7, pp. 163–217. Academic Press, New York (1971).
7. W. P. Teagan and G. S. Springer, Heat transfer and density distribution measurements between parallel plates in the transition regime, *Phys. Fluids* **11**, 497–506 (1968).
8. C. Cercignani, *Theory and Application of the Boltzmann Equation*. Scottish Academic Press, Edinburgh (1975).
9. S. J. O'Shea, Gas adsorption and heat transfer in evacuated collector tubes, Ph.D. Thesis, Sydney University (1989).
10. J. H. Ferziger and H. G. Kaper, *Mathematical Theory of Transport Processes in Gases*. North-Holland, Amsterdam (1972).
11. L. Lees and C. Liu, Kinetic theory description of conductive heat transfer from a fine wire, *Phys. Fluids* **5**, 1137–1148 (1962).
12. P. Bassanini, C. Cercignani and C. D. Pagani, Comparison of kinetic theory analyses of linearized heat transfer between parallel plates, *Int. J. Heat Mass Transfer* **10**, 447–460 (1967).
13. P. L. Bhatnagar, E. P. Gross and M. Krook, A model for collision processes in gases. I. Small amplitude processes in charged and neutral one-component systems, *Phys. Rev.* **94**, 511–525 (1954).
14. G. A. Bird, Monte Carlo simulation in an engineering context, *Prog. Astronaut. Aeronaut.* **74**, 239–255 (1981).
15. C. Borgnakke and P. S. Larsen, Statistical collision model for Monte Carlo simulation of polyatomic gas mixture, *J. Comput. Phys.* **18**, 405–420 (1975).
16. D. J. Evans and R. O. Watts, On the structure of liquid benzene, *Molec. Phys.* **32**, 83–96 (1976).
17. D. J. Evans and R. O. Watts, A theoretical study of transport coefficients in benzene vapor, *Molec. Phys.* **32**, 995–1015 (1976).
18. J. D. Lambert, *Vibrational and Rotational Relaxation in Gases*. Clarendon Press, Oxford (1977).
19. M. Rigby, E. B. Smith, W. A. Wakeham and G. C. Maitland, *The Forces Between Molecules*. Clarendon Press, Oxford (1986).
20. B. Stevens, *Collisional Activation in Gases*. Pergamon Press, Oxford (1967).
21. G. Herzberg, *Infrared and Raman Spectra of Polyatomic Molecules*. Van Nostrand, New York (1945).
22. R. C. Weast and M. J. Astle (Editors), *CRC Handbook of Chemistry and Physics*, 63rd Edn. CRC Press, Florida (1982).
23. J. P. Holman, *Heat Transfer*. McGraw-Hill, New York (1986).
24. F. O. Goodman and H. Y. Wachman, *Dynamics of Gas-surface Scattering*. Academic Press, New York (1976).
25. G. M. Rosenblatt, Translational and internal energy accommodation of molecular gases with solid surfaces, *Acc. Chem. Res.* **14**, 42–48 (1981).
26. S. K. Loyalka and J. R. Thomas, Heat transfer in a rarefied gas enclosed between parallel plates: role of boundary conditions, *Phys. Fluids* **25**, 1162–1164 (1982).
27. S. Craig and G. L. Harding, Structure, optical properties and decomposition kinetics of sputtered hydrogenated carbon, *Thin Solid Films* **97**, 345–361 (1982).
28. Y. G. Semyonov, S. F. Borisov and P. E. Suetin, Investigation of heat transfer in rarefied gases over a wide range of Knudsen number, *Int. J. Heat Mass Transfer* **27**, 1789–1799 (1984).
29. S. K. Hsu and T. F. Morse, Kinetic theory of parallel plate heat transfer in a polyatomic gas, *Phys. Fluids* **15**, 584–591 (1972).
30. N. Pazooki and S. K. Loyalka, Heat transfer in a rarefied polyatomic gas—1. Plane parallel plates, *Int. J. Heat Mass Transfer* **28**, 2019–2027 (1985); and Heat transfer in a rarefied polyatomic gas—2, *Sphere* **31**, 977–985 (1988).
31. J. W. Cipolla, Heat transfer and temperature jump in a polyatomic gas, *Int. J. Heat Mass Transfer* **14**, 1599–1610 (1971).